Environmental Science & Technology

Article

pubs.acs.org/est

Effect of Solar Radiation on the Optical Properties and Molecular Composition of Laboratory Proxies of Atmospheric Brown Carbon

Hyun Ji (Julie) Lee,[†] Paige Kuuipo Aiona,[†] Alexander Laskin,[‡] Julia Laskin,[§] and Sergey A. Nizkorodov*,[†]

[†]Department of Chemistry, University of California, Irvine, California 92697, United States

[‡]Environmental Molecular Sciences Laboratory and [§]Physical Sciences Division, Pacific Northwest National Laboratory, Richland, Washington 99352, United States

Supporting Information

ABSTRACT: Sources, optical properties, and chemical composition of atmospheric brown carbon (BrC) aerosol are uncertain, making it challenging to estimate its contribution to radiative forcing. Furthermore, optical properties of BrC may change significantly during its atmospheric aging. We examined the effect of photolysis on the molecular composition, mass absorption coefficient, and fluorescence of secondary organic aerosol (SOA) prepared by high-NO_x photooxidation of naphthalene (NAP SOA). Our experiments were designed to model photolysis processes of NAP SOA compounds dissolved in cloud or fog droplets. Aqueous solutions of NAP SOA were observed to photobleach (i.e., lose their ability to absorb visible radiation) with an effective half-life of ~15 h (with sun in its zenith) for the loss of near-UV (300−400 nm) absorbance. The molecular composition of NAP SOA was significantly modified by photolysis, with the average SOA formula changing from $C_{14.1}H_{14.5}O_{5.1}N_{0.085}$ to $C_{11.8}H_{14.9}O_{4.5}N_{0.023}$ after 4 h of irradiation. However, the average O/C ratio did not change significantly, suggesting that it is not a good metric for assessing the extent of photolysis-driven aging in NAP SOA (and in BrC in general). In contrast to NAP SOA, the photobleaching of BrC material produced by the reaction of limonene + ozone SOA with ammonia vapor (aged LIM/O_3 SOA) was much faster, but it did not result in a significant change in average molecular composition. The characteristic absorbance of the aged LIM/O_3 SOA in the 450−600 nm range decayed with an effective half-life of <0.5 h. These results emphasize the highly variable and dynamic nature of different types of atmospheric BrC.

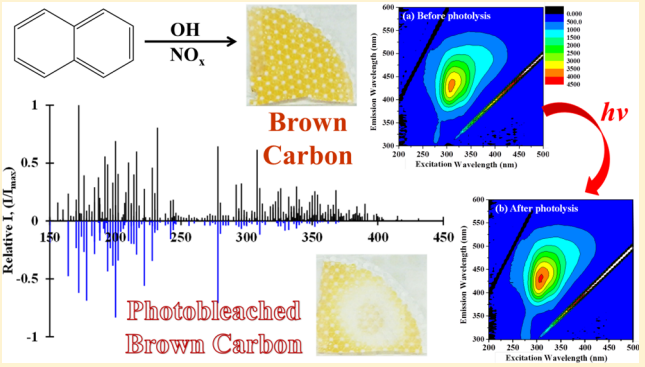

INTRODUCTION

Atmospheric aerosols affect the Earth's radiative balance by direct and indirect mechanisms.[1] The direct radiative forcing is typically negative (cooling) because light scattering dominates over absorption for most types of aerosols. However, aerosols that strongly absorb visible radiation, such as black carbon (BC), mineral dust, and brown carbon (BrC),[2] may either reduce the cooling effect or result in positive radiative forcing (warming).[3] In contrast to well characterized BC, the sources, optical properties, and chemical composition of BrC are not well understood, making it challenging to estimate the contribution of BrC to global forcing.[4−6]

Biomass burning and fossil-fuel combustion serve as important primary sources of BrC and BC. In addition, BrC may also have secondary sources related to gas-phase and aqueous processes involved in the formation and aging of secondary organic aerosols (SOA). For example, ammonium sulfate has been shown to react with glyoxal and methyl glyoxal in aqueous solutions producing imidazole-based light-absorbing compounds.[7−13] SOA produced from certain biogenic precursors, such as limonene (LIM), have been found to produce BrC in the presence of ammonia.[14−18] Aqueous oxidation of phenols and gas-phase oxidation of certain aromatic compounds also produce BrC material.[19−21] The multitude of poorly characterized secondary sources contributes to the challenge of constraining the properties of BrC aerosols in climate modeling.

Several studies demonstrated that optical properties of BrC may evolve significantly as a result of atmospheric aging. For example, Rincon et al. analyzed the absorption spectra of irradiated solutions of pyruvic acid and showed that the spectra change significantly depending on temperature, irradiation history, and other conditions.[22] Sareen et al. examined the properties of methyl glyoxal + ammonium sulfate reaction products and found that the near-UV absorbance of these products drops on a time scale of minutes in reactions with ozone and during photolysis.[11] Lambe et al. demonstrated that optical properties of SOA are strongly affected by extensive OH oxidation.[23] Zhong and Yang demonstrated that biomass

Received: May 22, 2014
Revised: August 6, 2014
Accepted: August 7, 2014
Published: August 7, 2014

Scheme 1. Initial Processes Involved in Atmospheric Oxidation of NAP Adapted and Modified from Nishino et al.[29a]

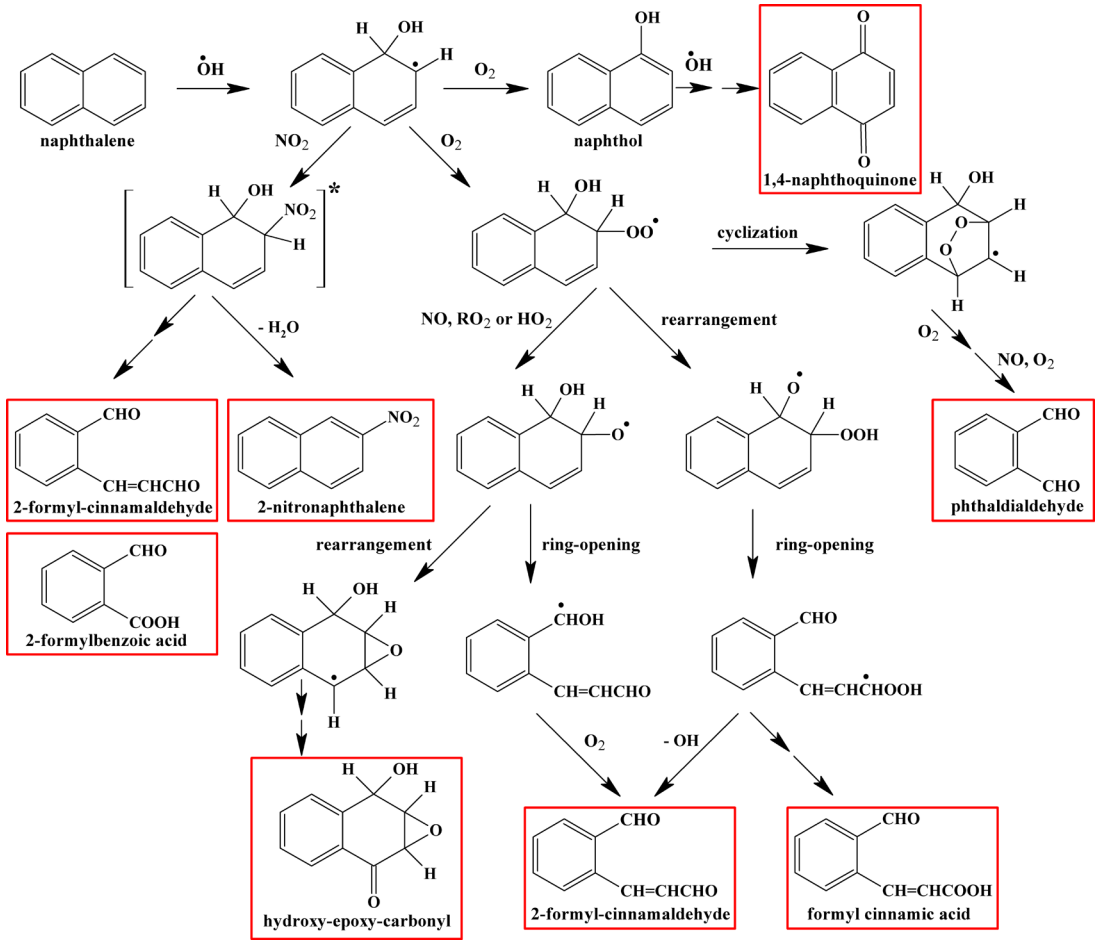

[a]In addition to the products retaining the NAP skeleton (naphthols and nitro compounds), a number of ring-opening benzene derivatives can also be produced. A partial list of possible products is provided in Table 1. Formulas corresponding to the boxed compounds have been observed in the HR-MS spectra reported in this work.

burning BrC undergoes reactions that both produce light-absorbing compounds and remove them on time scales of hours.[24] Therefore, it is not sufficient to know the initial absorption properties of BrC; it is also important to predict how they may evolve during various aging scenarios.

The goal of this study is to explore the effect of photolysis on the optical properties of laboratory generated proxies of BrC in aqueous solutions, as a model for cloud/fog processing of BrC. The model BrC used in this study is SOA produced by high-NO_x photooxidation of naphthalene (NAP). NAP is the most abundant and simplest polycyclic aromatic hydrocarbon found in highly populated urban areas,[24,25] with fossil-fuel combustion serving as its major source.[26−30] Gas-phase reaction with OH ($k = 2 \times 10^{-11}$ cm^3 $molecules^{-1}$ s^{-1})[26] is the primary sink for NAP resulting in a lifetime of about 6 h at $[OH] = 2 \times 10^6$ molecules cm^{-3}. This reaction forms a multitude of secondary pollutants in both the particle and gas phase. Scheme 1 shows the initial processes involved in NAP photooxidation, and Table 1 lists some of the products previously reported in the literature.[28−32] Some of the products shown in Scheme 1, such as aromatic aldehydes, nitroaromatic compounds, and quinones are expected to absorb light in the near-UV range and be photochemically active. Therefore, photolysis is expected to have a strong effect on NAP SOA composition.

NAP SOA can be considered a prototype of BrC material because of its relatively large absorption coefficient[18,23] and because its absorption spectrum is similar in shape to the absorption spectra of ambient organic and biomass burning aerosols.[24,33,34] In this work, we attempted to correlate the photolysis-driven changes in the optical properties of NAP SOA to changes in its molecular composition probed by high-resolution mass spectrometry (HR-MS). Photolysis produced significant changes in the molecular composition of NAP SOA but only had a modest effect on its wavelength-dependent mass absorption coefficient (MAC). To demonstrate that this is not universally applicable to all types of BrC, we also examined photolysis of BrC material produced by chemical aging of LIM/O_3 SOA with ammonia vapor (NH_3).[14,16−18] The aged LIM/O_3 SOA displayed the completely opposite behavior, with relatively small changes in the composition, but dramatic changes in the absorption spectrum. The contrast between NAP SOA and aged LIM/O_3 SOA emphasizes the highly variable and dynamic nature of different types of BrC materials.

EXPERIMENTAL METHODS

The methods are described in full in the Supporting Information and briefly summarized here. SOA samples were prepared by photooxidation of NAP in a 5 m^3 Teflon chamber under dry, high-NO_x conditions. Typical initial concentrations

Table 1. Partial List of Known Products of NAP Photooxidation

name[a]	formula	peak abundance (%) [M + H]$^+$	peak abundance (%) [M + Na]$^+$	effect of photolysis
benzoic acid	$C_7H_6O_2$			
phthaldialdehyde	$C_8H_6O_2$		37	↑
2-hydroxy benzoic acid	$C_7H_6O_3$			
phthalic anhydride	$C_8H_4O_3$			
2-formylbenzoic acid	$C_8H_6O_3$		13	↑
2-formyl-cinnamaldehyde	$C_{10}H_8O_2$	1.9	20	↓
formyl cinnamic acid	$C_{10}H_8O_3$	3.1	23	↑
naphthol	$C_{10}H_8O$			
1,4-naphthoquinone	$C_{10}H_6O_2$		2.4	↓
2,3-epoxy-1,4-quinone	$C_{10}H_6O_3$		6.4	↓
4-hydroxy-2,3-epoxy-carbonyl	$C_{10}H_7O_3$			
1-nitronaphthalene	$C_{10}H_7NO_2$		12	↓

[a]This table lists common names and chemical formulas of the products reported in refs 28−32. If the formula is detected in the unphotolyzed NAP SOA sample by ESI/HR-MS, the relative abundances (in % relative to the largest peak in the mass spectrum) of the corresponding protonated [M + H]$^+$ and sodiated [M + Na]$^+$ species are also included. The last column indicates whether the peaks corresponding to these compounds increase (↑) or are removed (↓) upon photolysis.

in the chamber were 450−900 ppb (10^{-9} by volume) of NAP, 500−800 ppb of NO, and 2−4 ppm (10^{-6} by volume) of H_2O_2. The steady-state OH concentration in the chamber ($\sim 5 \times 10^6$ molecules cm^{-3}) was estimated from the measured rate of decay of NAP and the known bimolecular rate constant (2×10^{-11} cm^3 molecules^{-1} s^{-1}) for the NAP + OH reaction.[26] After 3 h of photooxidation, SOA was collected on two PTFE filters (Millipore 0.2 μm pore size). The amount of SOA collected was estimated from scanning mobility particle sizer (SMPS) measurements assuming 100% collection efficiency by the filters and known NAP SOA density of 1.55 g cm^{-3}.[31] Typically, 800−1300 μg of SOA material was collected on each filter. In addition to the NAP SOA samples, SOA from ozonolysis of LIM (LIM/O_3 SOA) was generated and aged with NH_3 to produce BrC as described in Lee et al.[17] This type of aged SOA has a distinctive, well-characterized absorption spectrum in the visible range,[14,17,18,35] making it a convenient model system for studying photochemistry of BrC. We will refer to this material as "aged LIM/O_3 SOA" in the rest of this paper.

SOA was extracted from filters by sonication in 1.8−2 mL of deionized water for 10−15 min to achieve a concentration of 0.58 ± 0.07 mg mL^{-1} of dissolved SOA material. This concentration is considerably higher than typical levels of organic material in cloud droplets but comparable to concentrations in urban fogs and wet aerosols. Three-dimensional excitation−emission matrix (EEM) spectra of SOA extracts were acquired with a Hitachi F-4500 fluorescence spectrometer as described in Lee et al.[17] A dual-beam spectrometer (Shimadzu UV-2450) was used to record UV/vis absorption spectra of the SOA extracts. We observed that the absorption spectra of the NAP SOA extracts were pH dependent (Figure S1) and attribute the pH dependence to acid−base equilibria of nitrophenols. Spectra of nitrophenols are known to experience a significant red-shift upon ionization in solution.[36−38] The measured pH of the NAP SOA extracts were around 5−6, similar to the pH of cloud droplets.[39,40] Under these conditions, the degree of ionization of nitrophenols should be relatively small.

The procedure for the photolysis of aqueous SOA extracts in standard 1.0 cm quartz cuvettes was similar to that described by Epstein et al.[41] The radiant flux density was determined by photolyzing a 0.1 M solution of azoxybenzene (Fisher Scientific, 98%) in ethanol in the presence of 0.1 M potassium hydroxide (Figure S2).[41,42] Figure S3 shows a typical radiant flux density as a function of wavelength. Most of the photolyzing radiation fell in the 275−390 nm range with a maximum at 320 nm. The SOA photolysis experiments were repeated three times with independently generated SOA samples. In control experiments, a similar procedure was followed with the irradiation lamp turned off to confirm that the absorption spectra did not change significantly due to hydrolysis and other processes.

The SOA samples were analyzed with a high−resolution ($m/\Delta m \sim 10^5$ at m/z 450) linear-ion-trap (LTQ) Orbitrap mass spectrometer (Thermo Corp.) equipped with an electrospray ionization (ESI) source operating in the positive ion mode. In each set of experiments with independently prepared SOA samples, two identical SOA filter samples were separately extracted to obtain 0.34 ± 0.07 mg mL^{-1} SOA solutions in water. One of the solutions was photolyzed, while the other was kept in the dark as a control. The exposure was equivalent to about 3−4 h under a solar zenith angle (SZA) of 0°. The mass spectral data analysis was carried out as discussed in Nizkorodov et al.[43] Briefly, peaks that appeared in the blank sample and peaks corresponding to ^{13}C isotopes were discarded. The peaks were assigned to formulas $C_{1-40}H_{2-80}O_{0-35}N_{0-2}Na_{0-1}^+$ with 0.00075 m/z tolerance while constraining the H/C and O/C ratios to 0.4−2.5 and 0−1.0 and only permitting closed-shell ions (no ion-radicals).

RESULTS AND DISCUSSION

Mass Absorption Coefficients of NAP SOA. The measured absorption spectra presented in this work are in the form of wavelength-dependent MAC, which is calculated from the base-10 absorbance, A_{10}, of the SOA solution with known mass concentration, C_{mass} (g cm^{-3}), and path length, b (cm).[44]

$$\mathrm{MAC}(\lambda) = \frac{A_{10}^{solution}(\lambda) \times \ln(10)}{b \times C_{mass}} \quad (1)$$

Examples of the MAC spectra taken at different photolysis times are shown in Figure 1. The shapes of the spectra are characteristic of a typical atmospheric BrC material[34] and consistent with previous measurements for NAP SOA.[18,23] The absorption coefficient is highest in the UV range, but there is a broad tail in the visible range. The absolute MAC values (0−6000 cm^2 g^{-1} between 300−700 nm) are qualitatively consistent with previous measurements by Updyke et al. (0−5000 cm^2 g^{-1} in the same wavelength range).[18] The differences are likely due to uncertainties in estimating the mass of collected SOA from the SMPS data. A power law is customarily used to describe the wavelength dependence of the mass absorption coefficient of BrC, $\mathrm{MAC}(\lambda) = \mathrm{MAC}_o \times \lambda^{-AAE}$, where AAE stands for the absorption Angstrom exponent. Values of AAE in excess of 1, which are typical for BC-

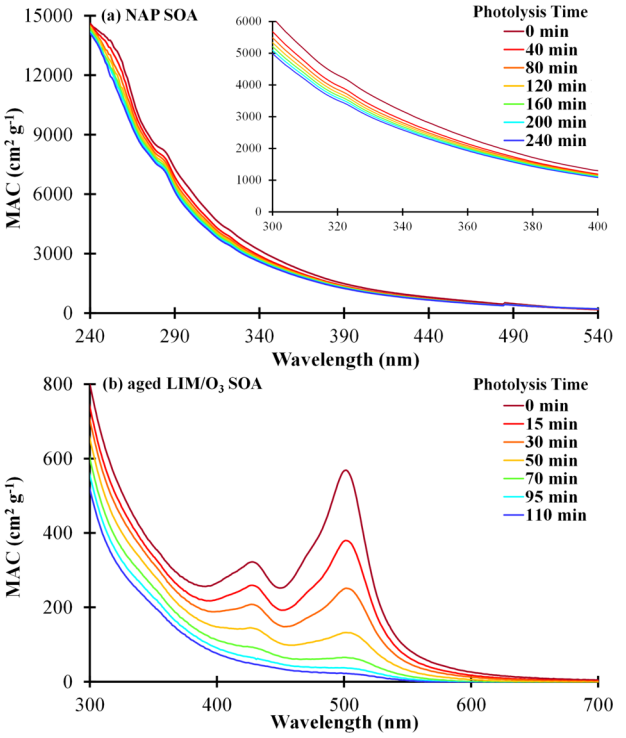

Figure 1. UV/vis absorption spectra recorded during photolysis of (a) an aqueous solution of NAP SOA and (b) an aqueous solution of LIM/O_3 SOA aged through reaction with ammonia vapor. The vertical axis corresponds to the mass absorption coefficient (MAC) calculated from eq 1. The inset in panel (a) zooms in on the 300−400 nm range.

dominated aerosol, indicate strong contribution of BrC to aerosol absorption. The *AAE* for NAP SOA studied here is ~6.2 for the visible wavelength range of 400−630 nm. It is slightly smaller than the value of 6.5 reported by Updyke et al. but closer to the range of reported *AAE* values for BrC, ranging from 2 to 7, measured in the field studies.[45−48] In summary, NAP SOA can be regarded as an example of a moderately−absorbing type of BrC.

Effective Rate of NAP SOA Photolysis. As Figure 1a demonstrates, the exposure of aqueous NAP SOA to actinic radiation slightly reduces its MAC, presumably as a result of photodegradation of BrC chromophores. Although omitted from Figure 1a, the MAC continues to decline at approximately the same rate upon further photolysis. Quantitative interpretation of these measurements is rather complicated because of the unknown and likely very large number of individual chromophores in the SOA solution. We approximate the MAC decay as a first-order kinetic process with an effective rate constant k.

$$\mathrm{MAC}_t = \mathrm{MAC}_0 \times \exp(-kt) \quad (2)$$

To facilitate the discussion of the atmospheric relevance of these results, we converted the laboratory photolysis time into an equivalent time in the atmosphere at SZA = 0°, as described in the Supporting Information. This procedure converts the photolysis rate resulting from irradiation by the UV source (shown in Figure S3) to that resulting from solar irradiation (also shown in Figure S3). We stress that this approach is approximate as it neglects wavelength dependence of the photolysis quantum yields for NAP SOA compounds.

Figure 2a shows the dependence of the average MAC in the near-UV (300−400 nm) and visible (450−600 nm) regions on

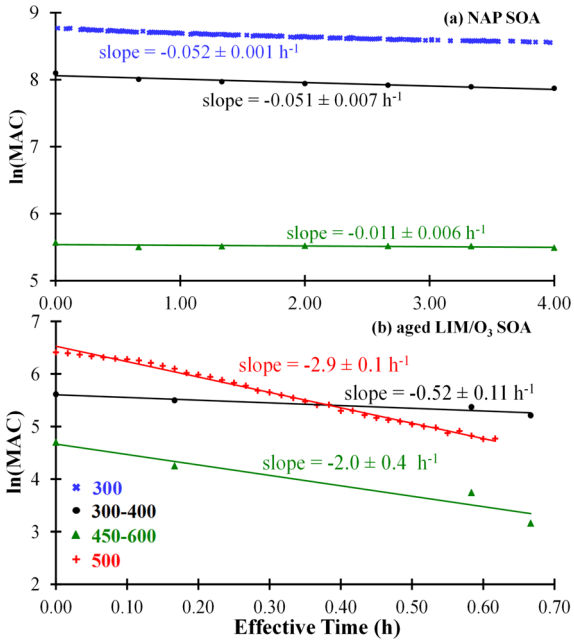

Figure 2. Decay of absorbance during irradiation of SOA aqueous solutions. (a) For NAP SOA, the average ln(MAC) is plotted against the effective photolysis time at 300 nm (blue x), in the near-UV region (300−400 nm, black points), and in the visible region (450−600 nm, green triangle). (b) For LIM/O_3 SOA + ammonia vapor reaction products, the data are plotted for the near-UV region, visible region, and at 500 nm (red +). The solid lines correspond to linear fits to the data. Numbers next to the lines correspond to the slopes $\pm 1\sigma$. The 300 nm measurement for NAP SOA and the 500 nm measurement for LIM/O_3 SOA were continuous single wavelength observation, while the rest were extracted from the individual absorption spectrum.

the effective atmospheric photolysis time. The effective rate constant, k, appears to be larger in the near-UV range (k = 0.052 h^{-1}) than in the visible range (k = 0.011 h^{-1}). These rates can be converted into empirical half-lives, $\tau = \ln(2)/k$, which are listed in Table 2. The half-life suggests that NAP SOA loses its ability to absorb near-UV and visible radiation on a time scale of days, with the fastest changes on the blue end of the spectrum. We verified in a separate set of experiments that NAP SOA can be completely photobleached (i.e., lose its yellow color) upon prolonged irradiation (after many effective days of photolysis).

Table 2. Effective Half-Life (in h) for the Disappearance of Absorbance at Different Wavelengths

wavelength (nm)[a]	NAP SOA	aged LIM/O_3 SOA
300	13	3.0
near-UV	14	1.3
visible	64	0.35
500	43	0.24

[a]The half-lives, $\tau = \ln(2)/k$, are calculated for NAP SOA and aged LIM/O_3 SOA at different regions: at 300 nm, in the near-UV region (300−400 nm), in the visible region (450−600 nm), and at 500 nm where the aged LIM/O_3 SOA has its characteristic absorption peak.

To demonstrate that not all BrC is as resilient to photolysis as NAP SOA, we also include data on photodegradation of BrC

produced by the reaction of LIM/O_3 SOA with NH_3.[6,17,18,49] Figure 1b shows the initial absorption spectrum of the aged LIM/O_3 SOA and its evolution during irradiation. The distinctive 500 nm peak is almost completely removed after 2 h of photolysis, and the brown color of the solution almost disappears in the process. The decay of MAC approximated by the first-order kinetics (Figure 2b) indicates an effective atmospheric photolysis time on the order of 1 h (Table 2). In contrast to NAP SOA, MAC changes faster in the visible range (k = 2.0 h^{-1}) than in the near-UV range (k = 0.52 h^{-1}).

Effect of Photolysis on Molecular Composition of Photolyzed NAP SOA. Table 1 lists known products of NAP photooxidation observed by gas chromatography−mass spectrometry,[28−30,32] proton-transfer-reaction mass spectrometry,[31] and aerosol mass spectrometry,[31,50,51] while Scheme 1 shows an abridged mechanism of their formation. Seven out of the 12 compounds listed in Table 1 appeared in the ESI/HR-MS spectra of NAP SOA, detected mostly as sodiated species. The expected major products[28−32,50,51] (phthaldialdehyde, formyl cinnamic acid, 2-formyl-cinnamaldehyde, 2-formylbenzoic acid, and 1-nitronaphthalene) were abundant in the mass spectra (10−40% of the largest observed peak). Other expected products were not detected, presumably because of relatively high volatility and low abundance in SOA (e.g., benzoic acid), lower ionization efficiencies, or possible hydrolysis in water extracts. For example, phthalic anhydride, a secondary oxidation product of phthaldialdehyde,[30,52] may have hydrolyzed in the aqueous solution.

Figure 3 compares the ESI high-resolution mass spectra acquired before and after photolysis of aqueous NAP SOA. For

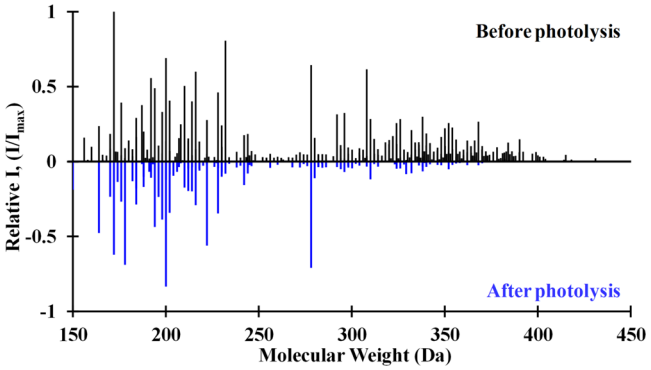

Figure 3. High-resolution positive ion mode mass spectra of NAP SOA before and after photolysis plotted as positive and negative signals, respectively. The spectra are normalized with respect to the largest detected peak. The preferential removal of larger compounds in photolysis is clearly evident from the spectra.

ease of comparison, the peak abundances are normalized to that of the largest peak in the corresponding mass spectrum. The initial mass spectrum had a bimodal peak distribution featuring the monomeric and dimeric groups of SOA constituents. Photolysis resulted in a significant change in the spectrum with the marked decline of the relative abundance of the dimeric compounds and parallel formation of new compounds at lower m/z values. Overall, before photolysis, 244 peaks (Table S1) were reproduced in all three NAP SOA samples (we only include peaks in our analysis that appeared in all three of the mass spectra of independently prepared samples). Of those, 150 peaks were removed by photolysis. In photolyzed samples, 108 peaks reproducibly appeared in all of the mass spectra. Of those, 14 peaks correspond to newly formed compounds, and 94 peaks correspond to compounds present in the initial sample. Clearly, photolysis affects the molecular composition of SOA in a profound way.

For an individual compound, $C_cH_hO_oN_n$, that contains c carbon, h hydrogen, o oxygen, and n nitrogen atoms, the double bond equivalent (DBE, the total number of double bonds and rings) can be calculated as follows:

$$\mathrm{DBE} = 1 + \frac{n - h}{2} + c \tag{3}$$

This formula assumes a valence of 3 for nitrogen, and therefore it underestimates the DBE for nitrocompounds (-NO_2) and organonitrates (-ONO_2) by 1. Figure 4a shows

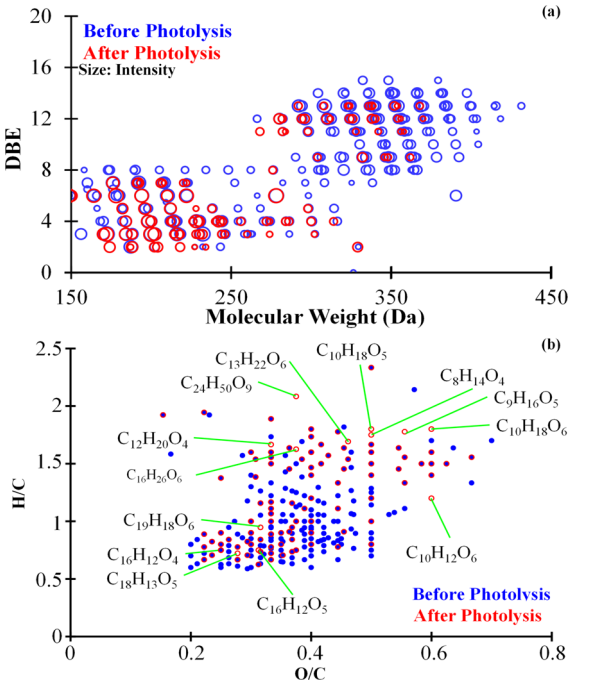

Figure 4. Comparison of molecular characteristics of the NAP SOA constituents before and after photolysis plotted as (a) DBE versus molecular weight (Da) and (b) Van Krevelen plot of H/C versus O/C.

the distribution of DBE values, which indicates a substantial decline in the DBE values upon photolysis presumably driven by the preferential destruction of larger, oligomeric compounds.

There is no clear effect of photolysis on the O/C or H/C ratios as evident from the lack of obvious patterns in the van Krevelen (VK) diagram (H/C vs O/C for individual compounds) in Figure 4b. In view of the molecular complexity of SOA, it is common to express its bulk composition as averaged elemental ratios. The average elemental composition and ratios (C, N, O, H/C, O/C, C/N, and O/N) and the average DBE can be estimated from the assigned molecular formulas:[53]

$$\langle Y \rangle = \frac{\sum_i x_i Y_i}{\sum_i x_i} \text{ where } Y = c,\ h,\ o,\ n,\ \text{or DBE} \tag{4}$$

dx.doi.org/10.1021/es502515r | Environ. Sci. Technol. 2014, 48, 10217−10226

Table 3. Average Elemental Composition, Elemental Ratios, and Double Bond Equivalents (DBE) before and after Photolysis of NAP SOA Solution

	⟨C⟩[a]	⟨H⟩	⟨O⟩	⟨N⟩	⟨H/C⟩	⟨O/C⟩	⟨N/C⟩	⟨N/O⟩	⟨DBE⟩
before (SD)	14.1	14.5	5.1	0.085	1.02	0.36	0.0060	0.017	7.9
	(0.7)	(0.4)	(0.1)	(0.017)	(0.06)	(0.02)	(0.0012)	(0.003)	(0.9)
after (SD)	11.8	14.9	4.5	0.023	1.27	0.38	0.0020	0.0053	5.3
	(0.4)	(0.6)	(0.3)	(0.003)	(0.07)	(0.03)	(0.0002)	(0.0007)	(0.2)
after − before	**−2.4**	**0.4**	**−0.7**	**−0.06**	**0.3**	**0.02**	**−0.0041**	**−0.012**	**−2.6**

[a]Data collected from three independent measurements were averaged. Errors are reported as 1σ standard deviation (SD) between the measurements.

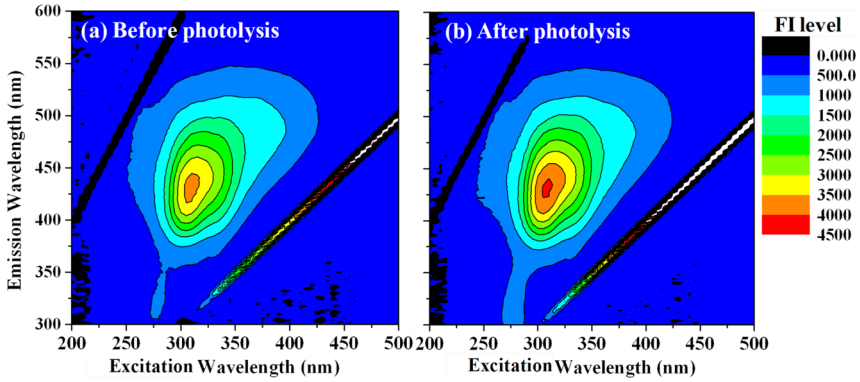

Figure 5. EEM spectrum recorded (a) before and (b) after photolysis. After 120 min of photolysis the fluorescence intensity (FI, color coded as shown on the right) increased somewhat (while the solution absorbance decreased, as shown in Figure 1).

$$\langle Y/Z\rangle = \frac{\sum_i x_i Y_i}{\sum_i x_i Z_i} \text{ where } Y/Z = \text{H/C, O/C, N/C, and N/O} \quad (5)$$

These formulas use peak abundances, x_i, as weighing factors. Strictly speaking, eq 5 calculates $\langle Y\rangle/\langle Z\rangle$, but we designate it as $\langle Y/Z\rangle$ to simplify the notation. Table 3 lists the elemental composition of NAP SOA before and after photolysis calculated using eqs 4 and 5. Based on these results, the 3−4 h of atmospheric photolysis of NAP SOA can be represented by an effective chemical equation:

$$C_{14.1}H_{14.5}O_{5.1}N_{0.085} + h\nu \rightarrow C_{11.8}H_{14.9}O_{4.5}N_{0.023} \quad (6)$$

The average carbon number, ⟨C⟩, as well as the overall molecular size, are reduced by photolysis. There is also a significant decrease in ⟨DBE⟩ implying a preferential breakdown of more unsaturated compounds. The average atomic ratios ⟨N/C⟩ and ⟨O/N⟩ drop in magnitude, while ⟨H/C⟩ increases. The small increase in ⟨H/C⟩ suggests a decrease in the level of unsaturation upon photolysis. It is noteworthy that the change in ⟨O/C⟩ is small (from 0.36 to 0.38). The ⟨O/C⟩ ratio, a measure of the degree of oxidation, is frequently used in the literature as an indicator of photochemical aging of SOA. Our results indicate that ⟨O/C⟩ may not be an informative parameter for tracking the age of SOA in cases when photolysis is the primary mechanism of aging.

Table S2 lists fractions of compounds containing 0 and 1 nitrogen atoms (0N and 1N compounds). The decrease in ⟨N⟩ and in the ⟨N/C⟩ ratio indicates a significant reduction in the fraction of 1N compounds during photolysis. Photolysis is known to be the dominant loss process for gas-phase nitronaphthalenes.[54] Our observations suggest that photolysis remains an important loss mechanism for these compounds in the aqueous phase. Indeed, the peak corresponding to nitronaphthalene (Table 1 and Table S1) disappears from the mass spectrum upon photolysis. Although nitroaromatic compounds have been shown to photodegrade very slowly in water,[55,52] they can be efficiently photoreduced in the presence of suitable hydrogen atom donors, such as alcohols and aldehydes,[56,57] which are abundant in SOA. Photoreduction of nitroaromatics is consistent with the observed decline in the N/O ratio of the products.

Another contribution to the loss of nitrogen-containing organics may come from photolysis of organonitrates, $RONO_2$, which are known to photolyze by breaking the weak O−N bond. Nguyen et al.[58] observed a significant reduction of organonitrates in the photolysis of aqueous solutions of high-NO_x isoprene SOA as well as formation of 2N species. In contrast to the isoprene SOA, we do not observe a buildup of 2N compounds after photolysis of NAP SOA. In fact, the fraction of 2N species both before and after photolysis was very small. This suggests that production of 2N compounds may be unique to the photolysis of high-NO_x isoprene SOA.

The known products of NAP photooxidation that do not contain nitrogen atoms (e.g., the ones shown in Table 1 and Scheme 1) were also strongly affected by photolysis. 2-Formylcinnamaldehyde was removed by photolysis in agreement with the expected reactivity of α,β-unsaturated aldehydes. Formyl cinnamic acid increased, presumably as a result of photooxidation of 2-formyl-cinnamaldehyde and similar compounds. Aromatic aldehydes, phthaldialdehyde and 2-formylbenzoic acid, both increased with photolysis. In summary, photolysis of NAP SOA introduces rather significant changes in its molecular composition.

To study the extent of compositional changes in aged LIM/O_3 SOA induced by photolysis, we carried out LC-ESI/HR-MS (reverse phase separation by liquid chromatography on a C18 column with the ESI/HR-MS detector) analysis before and

after photolysis. After 2 h photolysis of aged LIM/O_3 SOA, which was sufficient to completely change its absorption spectrum as shown in Figure 1b, the effective average chemical composition of SOA changed as follows:

$$C_{13.4}H_{19.1}O_{3.5}N_{0.62} + h\nu \rightarrow C_{14.2}H_{20.4}O_{4.3}N_{0.72} \quad (7)$$

Since a different technique was used to analyze the aged LIM/O_3 SOA and NAP SOA mixtures, a direct comparison to eq 6 cannot be made. However, this result shows that the extent of photolysis-driven changes in the mass spectra were smaller in the aged LIM/O_3 SOA than in NAP SOA. This result can be explained by the low relative abundance of the chromophores in aged LIM/O_3 SOA, which makes it difficult to detect them within a complex matrix of the much more abundant nonabsorbing compounds.[35]

Fluorescence of NAP SOA. The EEM spectra in Figure 5 show that NAP SOA was moderately fluorescent both before and after photolysis. The fluorescence quantum yield (QY), measured as described in Lee et al.,[17] increased from ∼0.2% to ∼0.3%. Although photolysis reduced the overall absorption coefficient of NAP SOA compounds (Figure 2), there was a slight increase in their fluorescence intensity as shown in Figure 5b. This is an unexpected result, considering that the photolysis of NAP SOA also reduced the average number of double bonds (inferred from DBE values) in the NAP SOA sample (Figure 4 and Table 3), thus preferentially removing highly unsaturated molecules that are more likely to fluoresce. One possible contribution to the increased fluorescence intensity is the loss of nitroaromatic compounds during photolysis. Such compounds undergo highly efficient intersystem crossing (ISC) into the triplet manifold, followed by thermal relaxation.[59] Shutting down the ISC pathway could make the effective QY higher. Another possibility is that the photolysis may create carboxylic acids and reduce the solution pH. This was observed as the typical starting NAP SOA pH of about 5−6 decreased by 0−1 units during photolysis. When we carried out fluorescence measurements on unphotolyzed samples at intentionally lowered pH values, we also observed higher emissions intensities. Therefore, some of the observed increase in the fluorescence intensity may be attributed to the pH effects. We note that the observed increase in the intensity of fluorescence in the photolyzed NAP SOA is in stark contrast with the aged LIM/O_3 SOA system, which loses its ability to fluoresce upon photolysis. Figure S4 in the Supporting Information shows a typical EEM spectrum for the aged LIM/O_3 SOA solution before and after photolysis.

Atmospheric Implications. We examined the photolysis of aqueous solutions of NAP SOA, a prototypical BrC aerosol, as a model of photochemical processing of BrC compounds in cloud and fog droplets. Photolysis had a modest effect on the wavelength-dependent MAC of NAP SOA but produced significant changes in the molecular composition as determined by ESI/HR-MS methods. To demonstrate that this is not universally applicable to all types of BrC, we also presented results on the photolysis of BrC produced by reaction of LIM/O_3 SOA aged with NH_3. This system displayed an opposite behavior to NAP SOA, with relatively little change in the overall composition, but more dramatic and faster changes in the absorption spectrum. These results highlight the great diversity of properties of different types of BrC and imply that the chemical nature of the light-absorbing compounds in different types of BrC can be quite different.

An important conclusion of this work is that chemical composition and optical properties of BrC cannot be viewed as static. Light-absorbing compounds responsible for the color of BrC can potentially photobleach in sunlight (i.e., lose their ability to absorb visible radiation). This photobleaching can be quite fast, as in the case of light-absorbing products of reactions of LIM/O_3 SOA + NH_3 (a couple of hours of irradiation, Figure 2) and methyl glyoxal + ammonium sulfate (a few minutes of irradiation according to the estimation in Sareen et al.[11]). It can also be considerably slower, as in the case of NAP SOA examined in this work. Our conclusions corroborate the results of Zhong and Jang, who found that the absorption spectrum of biomass-burning aerosol changed significantly over the course of a day due to a competition between formation and photobleaching of light-absorbing organics.[24]

Even in the case of the relatively resilient NAP SOA, the MAC decays with an estimated effective half-life of ∼15 h. Therefore, in addition to the wavelength-dependent MAC values of various BrC samples, the effective rate with which MAC evolves under typical atmospheric conditions should also be quantified and reported. A strongly absorbing BrC sample will not produce much direct radiative forcing if it photolyzes in minutes, as reported, for example, for the chromophores in methyl glyoxal + ammonium sulfate solutions.[11]

The average O/C ratio is a parameter that can be derived from aerosol mass spectrometry measurements.[60,61] In many reports, O/C is used as a convenient indicator of the degree of oxidation in SOA, and a number of studies have attempted to correlate O/C with the aerosol type, chemical age, and even its properties, such as viscosity, optical properties,[23] hygroscopicity,[62,63] etc. Our results suggest that the O/C ratio is not a fundamental characteristic that can uniquely describe these SOA properties. The chemical composition and MAC of NAP SOA undergoes significant changes during photolysis. However, these changes cannot be adequately captured by bulk measurements of the O/C ratio. Therefore, this type of photolysis-driven aging would likely be missed by measurements of integrated O/C values.

Although this work focused on aqueous solutions of NAP SOA, we also briefly examined photolysis of NAP SOA material directly on the filter. The photolysis also resulted in efficient photobleaching (photographs of NAP SOA filters before and after photolysis are shown in the Table of Contents image in the abstract). Moreover, the molecular composition of NAP SOA photolyzed on the filter changed in a qualitatively similar manner to that in an aqueous NAP SOA solution. Therefore, the scope of our results is not limited to aqueous photolysis of SOA; photolysis is likely to be just as important in organic particles (although the mechanism of photolysis in the aerosol may be very different from that in the aqueous solution of SOA). This is consistent with our previous observations of efficient photochemistry of biogenic SOA material.[64−66]

Finally, a significant fluorescence level of NAP SOA, with QY of ∼0.2−0.3%, is worth noting. Many studies have reported strong fluorescence emission produced by primary biological aerosol particles (PBAP).[67−69] Lee et al. suggested that SOA may interfere with detection of PBAP with fluorescence-based techniques. The wide excitation (250−425 nm) and emission (350−550 nm) range for NAP SOA further supports this concern. In fact, the emission of NAP SOA overlaps even better with the EEM peak for PBAP than that of the biogenic SOA reported previously in Lee et al.[17]

■ ASSOCIATED CONTENT

Supporting Information

Additional experimental details, data on pH dependence of the absorption spectrum of NAP SOA, description of calculation of the radiant flux densities using actinometer measurements, comparison of the radiant flux density from the photolysis source and from the sun, description of the calculation of the effective photolysis rate under ambient conditions, a detailed list of compounds removed/formed/remaining during photolysis of aqueous NAP SOA, and a breakdown of these compounds into N1 and N2 species. This material is available free of charge via the Internet at http://pubs.acs.org.

■ AUTHOR INFORMATION

Corresponding Author

*Phone: 949-824-1262. Fax: (949) 824-8571. E-mail: nizkorod@uci.edu.

Notes

The authors declare no competing financial interest.

■ ACKNOWLEDGMENTS

We acknowledge support by the U.S. Department of Commerce, National Oceanic and Atmospheric Administration through Climate Program Office's AC4 program, awards NA13OAR4310066 (PNNL) and NA13OAR4310062 (UCI). H.J.L. acknowledges support by the NSF grant AGS-1227579. The ESI/HR-MS analysis was performed at the W.R. Wiley Environmental Molecular Sciences Laboratory (EMSL) - a national scientific user facility located at PNNL - and sponsored by the Office of Biological and Environmental Research of the U.S. PNNL is operated for US DOE by Battelle Memorial Institute under Contract No. DE-AC06-76RL0 1830.

■ REFERENCES

(1) Solomon, S. Q. D.; Manning, M.; Chen, Z.; Marquis, M.; Averyt, K.; Tignor, M.; Miller, H. L. In *Contribution of Working Group I to the Fourth Assessment Report of the Intergovernmental Panel on Climate Change*; New York, 2007.

(2) Andreae, M. O.; Gelencser, A. Black carbon or brown carbon? The nature of light-absorbing carbonaceous aerosols. *Atmos. Chem. Phys.* **2006**, *6* (10), 3131−3148.

(3) Ramanathan, V.; Carmichael, G. Global and regional climate changes due to black carbon. *Nat. Geosci.* **2008**, *1* (4), 221−227.

(4) Alexander, D. T. L.; Crozier, P. A.; Anderson, J. R. Brown carbon spheres in east asian outflow and their optical properties. *Science* **2008**, *321* (5890), 833−836.

(5) Bahadur, R.; Praveen, P. S.; Xu, Y.; Ramanathan, V. Solar absorption by elemental and brown carbon determined from spectral observations. *Proc. Nat. Acad. Sci.* **2012**, *109* (43), 17366−17371.

(6) Bond, T. C.; Bergstrom, R. W. Light Absorption by Carbonaceous Particles: An Investigative Review. *Aerosol Sci. Technol.* **2006**, *40* (1), 27−67.

(7) Aregahegn, K. Z.; Noziere, B.; George, C. Organic aerosol formation photo-enhanced by the formation of secondary photosensitizers in aerosols. *Faraday Discuss.* **2013**, *165*, 123−134.

(8) De Haan, D. O.; Corrigan, A. L.; Tolbert, M. A.; Jimenez, J. L.; Wood, S. E.; Turley, J. J. Secondary Organic Aerosol Formation by Self-Reactions of Methylglyoxal and Glyoxal in Evaporating Droplets. *Environ. Sci. Technol.* **2009**, *43* (21), 8184−8190.

(9) Kampf, C. J.; Jakob, R.; Hoffmann, T. Identification and characterization of aging products in the glyoxal/ammonium sulfate system-implications for light-absorbing material in atmospheric aerosols. *Atmos. Chem. Phys.* **2012**, *12* (14), 6323−6333.

(10) Noziere, B.; Cordova, A. A kinetic and mechanistic study of the amino acid catalyzed aldol condensation of acetaldehyde in aqueous and salt solutions. *J. Phys. Chem. A* **2009**, *112* (13), 2827−2837.

(11) Sareen, N.; Schwier, A. N.; Shapiro, E. L.; Mitroo, D.; McNeill, V. F. Secondary organic material formed by methylglyoxal in aqueous aerosol mimics. *Atmos. Chem. Phys.* **2010**, *10* (3), 997−1016.

(12) Shapiro, E. L.; Szprengiel, J.; Sareen, N.; Jen, C. N.; Giordano, M. R.; McNeill, V. F. Light-absorbing secondary organic material formed by glyoxal in aqueous aerosol mimics. *Atmos. Chem. Phys.* **2009**, *9*, 2289−2300.

(13) Trainic, M.; Abo Riziq, A.; Lavi, A.; Flores, J. M.; Rudich, Y. The optical, physical and chemical properties of the products of glyoxal uptake on ammonium sulfate seed aerosols. *Atmos. Chem. Phys.* **2011**, *11* (18), 9697−9707.

(14) Bones, D. L.; Henricksen, D. K.; Mang, S. A.; Gonsior, M.; Bateman, A. P.; Nguyen, T. B.; Cooper, W. J.; Nizkorodov, S. A. Appearance of strong absorbers and fluorophores in limonene-O_3 secondary organic aerosol due to NH_4^+-mediated chemical aging over long time scales. *J. Geophys. Res.* **2010**, *115*, (D5), doi: 10.1029/2009JD012864.

(15) Flores, J. M.; Washenfelder, R. A.; Adler, G.; Lee, H. J.; Segev, L.; Laskin, J.; Laskin, A.; Nizkorodov, S. A.; Brown, S. S.; Rudich, Y. Complex refractive indices in the near-ultraviolet spectral region of biogenic secondary organic aerosol aged with ammonia. *Phys. Chem. Chem. Phys.* **2014**, *16* (22), 10629−10642.

(16) Laskin, J.; Eckert, P. A.; Roach, P. J.; Heath, B. S.; Nizkorodov, S. A.; Laskin, A. Chemical analysis of complex organic mixtures using reactive nanospray desorption electrospray ionization mass spectrometry. *Anal. Chem.* **2012**, *84* (16), 7179−7187.

(17) Lee, H. J.; Laskin, A.; Laskin, J.; Nizkorodov, S. A. Excitation−emission spectra and fluorescence quantum yields for fresh and aged biogenic secondary organic aerosols. *Environ. Sci. Technol.* **2013**, *47* (11), 5763−5770.

(18) Updyke, K. M.; Nguyen, T. B.; Nizkorodov, S. A. Formation of brown carbon via reactions of ammonia with secondary organic aerosols from biogenic and anthropogenic precursors. *Atmos. Environ.* **2012**, *63*, 22−31.

(19) Chang, J. L.; Thompson, J. E. Characterization of colored products formed during irradiation of aqueous solutions containing H_2O_2 and phenolic compounds. *Atmos. Environ.* **2010**, *44* (4), 541−551.

(20) Gelencsér, A.; Hoffer, A.; Kiss, G.; Tombácz, E.; Kurdi, R.; Bencze, L. In-situ formation light-absorbing organic matter in cloud water. *J. Atmos. Chem.* **2003**, *45* (1), 25−33.

(21) Jacobson, M. Z. Isolating nitrated and aromatic aerosols and nitrated aromatic gases as sources of ultraviolet light absorption. *J. Geophys. Res.* **1999**, *104* (D3), 3527−3542.

(22) Rincón, A. G.; Guzmán, M. I.; Hoffmann, M. R.; Colussi, A. J. Thermochromism of model organic aerosol matter. *J. Phys. Chem. Lett.* **2009**, *1* (1), 368−373.

(23) Lambe, A. T.; Cappa, C. D.; Massoli, P.; Onasch, T. B.; Forestieri, S. D.; Martin, A. T.; Cummings, M. J.; Croasdale, D. R.; Brune, W. H.; Worsnop, D. R.; Davidovits, P. Relationship between oxidation level and optical properties of secondary organic aerosol. *Environ. Sci. Technol.* **2013**, *47* (12), 6349−6357.

(24) Zhong, M.; Jang, M. Dynamic light absorption of biomass-burning organic carbon photochemically aged under natural sunlight. *Atmos. Chem. Phys.* **2014**, *14* (3), 1517−1525.

(25) Desyaterik, Y.; Sun, Y.; Shen, X.; Lee, T.; Wang, X.; Wang, T.; Collett, J. L. Speciation of "brown" carbon in cloud water impacted by agricultural biomass burning in eastern China. *J. Geophys. Res: Atmos.* **2013**, *118* (13), 7389−7399.

(26) Atkinson, R.; Arey, J. Atmospheric chemistry of gas-phase polycyclic aromatic hydrocarbons: formation of atmospheric mutagens. *Environ. Health Perspect.* **1994**, *102* (Suppl 4), 117−26.

(27) Atkinson, R.; Arey, J. Mechanisms of the gas-phase reactions of aromatic hydrocarbons and PAHs with OH and NO_3 radicals. *Polycyclic Aromat. Compd.* **2007**, *27* (1), 15−40.

(28) Bunce, N. J.; Liu, L.; Zhu, J.; Lane, D. A. Reaction of naphthalene and its derivatives with hydroxyl radicals in the gas phase. *Environ. Sci. Technol.* **1997**, *31* (8), 2252−2259.
(29) Nishino, N.; Arey, J.; Atkinson, R. 2-Formylcinnamaldehyde formation yield from the OH radical-initiated reaction of naphthalene: effect of NO_2 concentration. *Environ. Sci. Technol.* **2012**, *46* (15), 8198−8204.
(30) Wang, L.; Atkinson, R.; Arey, J. Dicarbonyl products of the OH radical-initiated reactions of naphthalene and the C1- and C2-alkylnaphthalenes. *Environ. Sci. Technol.* **2007**, *41* (8), 2803−2810.
(31) Chan, A. W. H.; Kautzman, K. E.; Chhabra, P. S.; Surratt, J. D.; Chan, M. N.; Crounse, J. D.; Kürten, A.; Wennberg, P. O.; Flagan, R. C.; Seinfeld, J. H. Secondary organic aerosol formation from photooxidation of naphthalene and alkylnaphthalenes: implications for oxidation of intermediate volatility organic compounds (IVOCs). *Atmos. Chem. Phys.* **2009**, *9* (9), 3049−3060.
(32) Sasaki, J.; Aschmann, S. M.; Kwok, E. S. C.; Atkinson, R.; Arey, J. Products of the gas-phase OH and NO_3 radical-initiated reactions of naphthalene. *Environ. Sci. Technol.* **1997**, *31* (11), 3173−3179.
(33) Hecobian, A.; Zhang, X.; Zheng, M.; Frank, N.; Edgerton, E. S.; Weber, R. J. Water-soluble organic aerosol material and the light-absorption characteristics of aqueous extracts measured over the Southeastern United States. *Atmos. Chem. Phys.* **2010**, *10* (13), 5965−5977.
(34) Sun, H.; Biedermann, L.; Bond, T. C. Color of brown carbon: A model for ultraviolet and visible light absorption by organic carbon aerosol. *Geophys. Res. Lett.* **2007**, *34* (17), L17813.
(35) Laskin, J.; Laskin, A.; Roach, P. J.; Slysz, G. W.; Anderson, G. A.; Nizkorodov, S. A.; Bones, D. L.; Nguyen, L. Q. High-Resolution Desorption Electrospray Ionization Mass Spectrometry for Chemical Characterization of Organic Aerosols. *Anal. Chem.* **2010**, *82* (5), 2048−2058.
(36) Vione, D.; Maurino, V.; Minero, C.; Duncianu, M.; Olariu, R.-I.; Arsene, C.; Sarakha, M.; Mailhot, G. Assessing the transformation kinetics of 2- and 4-nitrophenol in the atmospheric aqueous phase. Implications for the distribution of both nitroisomers in the atmosphere. *Atmos. Environ.* **2009**, *43* (14), 2321−2327.
(37) Hayon, E.; Ibata, T.; Lichtin, N. N.; Simic, M. Electron and hydrogen atom attachment to aromatic carbonyl compounds in aqueous solution. Absorption spectra and dissociation constants of ketyl radicals. *J. Phys. Chem.* **1972**, *76* (15), 2072−2078.
(38) Zhu, D.; Hyun, S.; Pignatello, J. J.; Lee, L. S. Evidence for $\pi-\pi$ electron donor−acceptor interactions between π-donor aromatic compounds and π-acceptor sites in soil organic matter through pH effects on sorption. *Environ. Sci. Technol.* **2004**, *38* (16), 4361−4368.
(39) Brantner, B.; Fierlinger, H.; Puxbaum, H.; Berner, A. Cloudwater chemistry in the subcooled droplet regime at Mount Sonnblick (3106 M A.S.L., Salzburg, Austria). *Water, Air, Soil Pollut.* **1994**, *74* (3−4), 363−384.
(40) Marinoni, A.; Parazols, M.; Brigante, M.; Deguillaume, L.; Amato, P.; Delort, A.-M.; Laj, P.; Mailhot, G. Hydrogen peroxide in natural cloud water: Sources and photoreactivity. *Atmos. Res.* **2011**, *101* (1−2), 256−263.
(41) Epstein, S. A.; Shemesh, D.; Tran, V. T.; Nizkorodov, S. A.; Gerber, R. B. Absorption spectra and photolysis of methyl peroxide in liquid and frozen water. *J. Phys. Chem. A* **2012**, *116* (24), 6068−6077.
(42) Bunce, N. J.; Lamarre, J.; Vaish, S. P. Photorearrangment of azoxybenzene to 2-hydroxyazobenezene: A convenient chemical actinometer. *Photochem. Photobiol.* **1984**, *39* (4), 531−533.
(43) Nizkorodov, S. A.; Laskin, J.; Laskin, A. Molecular chemistry of organic aerosols through the application of high resolution mass spectrometry. *Phys. Chem. Chem. Phys.* **2011**, *13* (9), 3612−3629.
(44) Chen, Y.; Bond, T. C. Light absorption by organic carbon from wood combustion. *Atmos. Chem. Phys.* **2010**, *10*, 1773−1787.
(45) Bergstrom, R. W.; Pilewskie, P.; Russell, P. B.; Redemann, J.; Bond, T. C.; Quinn, P. K.; Sierau, B. Spectral absorption properties of atmospheric aerosols. *Atmos. Chem. Phys.* **2007**, *7* (23), 5937−5943.
(46) Pöschl, U. Aerosol particle analysis: challenges and progress. *Anal. Bioanal. Chem.* **2003**, *375* (1), 30−32.
(47) Hoffer, A.; Gelencsér, A.; Guyon, P.; Kiss, G.; Schmid, O.; Frank, G. P.; Artaxo, P.; Andreae, M. O. Optical properties of humic-like substances (HULIS) in biomass-burning aerosols. *Atmos. Chem. Phys.* **2006**, *6* (11), 3563−3570.
(48) Kirchstetter, T. W.; Thatcher, T. L. Contribution of organic carbon to wood smoke particulate matter absorption of solar radiation. *Atmos. Chem. Phys. Discuss.* **2012**, *12* (2), 5803−5816.
(49) Nguyen, T. B.; Laskin, A.; Laskin, J.; Nizkorodov, S. A. Direct aqueous photochemistry of isoprene high-NOx secondary organic aerosol. *Phys. Chem. Chem. Phys.* **2012**, *14* (27), 9702−9714.
(50) Chhabra, P. S.; Ng, N. L.; Canagaratna, M. R.; Corrigan, A. L.; Russell, L. M.; Worsnop, D. R.; Flagan, R. C.; Seinfeld, J. H. Elemental composition and oxidation of chamber organic aerosol. *Atmos. Chem. Phys.* **2011**, *11* (17), 8827−8845.
(51) McWhinney, R. D.; Zhou, S.; Abbatt, J. P. D. Naphthalene SOA: redox activity and naphthoquinone gas−particle partitioning. *Atmos. Chem. Phys.* **2013**, *13* (19), 9731−9744.
(52) Calvert, J. G.; Mellouki, A.; Orlando, J. J.; Pilling, M. J.; Willington, T. J. *The Mechanisms of Atmospheric Oxidation of The Oxygenates*; Oxford University Press, Inc.: New York, 2011.
(53) Bateman, A. P.; Laskin, J.; Laskin, A.; Nizkorodov, S. A. Applications of high-resolution electrospray ionization mass spectrometry to measurements of average oxygen to carbon ratios in secondary organic aerosols. *Environ. Sci. Technol.* **2012**, *46* (15), 8315−8324.
(54) Atkinson, R.; Aschmann, S. M.; Arey, J.; Barbara, Z.; Schuetzle, D. Gas-phase atmospheric chemistry of 1- and 2-nitronaphthalene and 1,4-naphthoquinone. *Atmos. Environ. (1967−1989)* **1989**, *23* (12), 2679−2690.
(55) Lipczynska-Kochany, E. Degradation of nitrobenzene and nitrophenols in homogeneous aqueous solution. Direct photolysis versus photolysis in the presence of hydrogen peroxide and the Fenton reagent. *Water Pollut. Res. J. Canada* **1992**, *27* (1), 97−122.
(56) Barltrop, J. A.; Bunce, N. J. Organic photochemistry. Part VIII. The photochemical reduction of nitro-compounds. *J. Chem. Soc. C* **1968**, No. 0, 1467−1474.
(57) Hashimoto, S.; Kano, K. The photochemical reduction of nitrobenzene and its reduction intermediates. X. The photochemical reduction of the monosubstituted nitrobenzenes in 2-propanol. *Bull. Chem. Soc. Jpn.* **1972**, *45* (2), 549−553.
(58) Nguyen, T. B.; Lee, P. B.; Updyke, K. M.; Bones, D. L.; Laskin, J.; Laskin, A.; Nizkorodov, S. A. Formation of nitrogen- and sulfur-containing light-absorbing compounds accelerated by evaporation of water from secondary organic aerosols. *J. Geophys. Res.: Atmos.* **2012**, *117*, (D1), doi: 10.1029/2011JD016944.
(59) Takezaki, M.; Hirota, N.; Terazima, M. Nonradiative relaxation processes and electronically excited states of nitrobenzene studied by picosecond time-resolved transient grating method. *J. Phys. Chem. A* **1997**, *101* (19), 3443−3448.
(60) Aiken, A. C.; DeCarlo, P. F.; Jimenez, J. L. Elemental analysis of organic species with electron ionization high-resolution mass spectrometry. *Anal. Chem.* **2007**, *79* (21), 8350−8358.
(61) Aiken, A. C.; DeCarlo, P. F.; Kroll, J. H.; Worsnop, D. R.; Huffman, J. A.; Docherty, K. S.; Ulbrich, I. M.; Mohr, C.; Kimmel, J. R.; Sueper, D.; Sun, Y.; Zhang, Q.; Trimborn, A.; Northway, M.; Ziemann, P. J.; Canagaratna, M. R.; Onasch, T. B.; Alfarra, M. R.; Prevot, A. S. H.; Dommen, J.; Duplissy, J.; Metzger, A.; Baltensperger, U.; Jimenez, J. L. O/C and OM/OC ratios of primary, secondary, and ambient organic aerosols with high-resolution time-of-flight aerosol mass spectrometry. *Environ. Sci. Technol.* **2008**, *42* (12), 4478−4485.
(62) Duplissy, J.; DeCarlo, P. F.; Dommen, J.; Alfarra, M. R.; Metzger, A.; Barmpadimos, I.; Prevot, A. S. H.; Weingartner, E.; Tritscher, T.; Gysel, M.; Aiken, A. C.; Jimenez, J. L.; Canagaratna, M. R.; Worsnop, D. R.; Collins, D. R.; Tomlinson, J.; Baltensperger, U. Relating hygroscopicity and composition of organic aerosol particulate matter. *Atmos. Chem. Phys.* **2011**, *11* (3), 1155−1165.
(63) Stock, M.; Cheng, Y. F.; Birmili, W.; Massling, A.; Wehner, B.; Müller, T.; Leinert, S.; Kalivitis, N.; Mihalopoulos, N.; Wiedensohler, A. Hygroscopic properties of atmospheric aerosol particles over the Eastern Mediterranean: implications for regional direct radiative

forcing under clean and polluted conditions. *Atmos. Chem. Phys.* **2011**, *11* (9), 4251−4271.
(64) Mang, S. A.; Henricksen, D. K.; Bateman, A. P.; Andersen, M. P. S.; Blake, D. R.; Nizkorodov, S. A. Contribution of carbonyl photochemistry to aging of atmospheric secondary organic aerosol. *J. Phys. Chem. A* **2008**, *112* (36), 8337−8344.
(65) Pan, X.; Underwood, J. S.; Xing, J. H.; Mang, S. A.; Nizkorodov, S. A. Photodegradation of secondary organic aerosol generated from limonene oxidation by ozone studied with chemical ionization mass spectrometry. *Atmos. Chem. Phys.* **2009**, *9* (12), 3851−3865.
(66) Walser, M. L.; Park, J.; Gomez, A. L.; Russell, A. R.; Nizkorodov, S. A. Photochemical aging of secondary organic aerosol particles generated from the oxidation of d-limonene. *J. Phys. Chem. A* **2007**, *111* (10), 1907−1913.
(67) Ammor, M. Recent advances in the use of intrinsic fluorescence for bacterial identification and characterization. *J. Fluoresc.* **2007**, *17* (5), 455−459.
(68) Hill, S. C.; Pinnick, R. G.; Niles, S.; Pan, Y.-L.; Holler, S.; Chang, R. K.; Bottiger, J.; Chen, B. T.; Orr, C.-S.; Feather, G. Real-time measurement of fluorescence spectra from single airborne biological particles. *Anal. Chem. Technol.* **1999**, *3* (4−5), 221−239.
(69) Pöhlker, C.; Huffman, J. A.; Pöschl, U. Autofluorescence of atmospheric bioaerosols − fluorescent biomolecules and potential interferences. *Atmos. Meas. Technol.* **2012**, *5*, 37−71.